

## Electronic Supplementary Information

# Synergic Nanoantioxidant Based on Covalently Modified Halloysite-Trolox Nanotubes with Intralumen Loaded Quercetin

*Marina Massaro,<sup>†</sup> Serena Riela,<sup>†\*</sup> Susanna Guernelli<sup>§</sup>, Filippo Parisi,<sup>#</sup> Giuseppe Lazzara,<sup>#</sup> Andrea Baschieri,<sup>§</sup> Luca Valgimigli,<sup>§</sup> Riccardo Amorati<sup>§\*</sup>*

<sup>†</sup>University of Palermo, Department STEBICEF, section Chemistry, Viale delle Scienze, Ed. 17, I-90128 Palermo, Italy. <sup>§</sup>University of Bologna, Department of Chemistry “G. Ciamician”, Via S. Giacomo 11, I-40126 Bologna, Italy. <sup>#</sup>University of Palermo, Department of Physics and Chemistry, Viale delle Scienze, Parco d'Orleans II, Ed. 17, 90128 Palermo, Italy.

<b>Content</b>	<b>page</b>
Figure S1. IR spectrum of HNT-Trolox	2
Figures S2-S3. Thermogravimetric curves	3
Figures S4-S8. UV-vis spectra of the reaction with DPPH•	4
Figure S9. Release profile of quercetin from HNT/Que	6
Procedure of numerical fitting	7
Figures S10-S11. Results from numerical fittings.	10
Figure S12. Antioxidant activity of Trolox – quercetin mixture	12
Figure S13. Fluorescence emission spectra	12

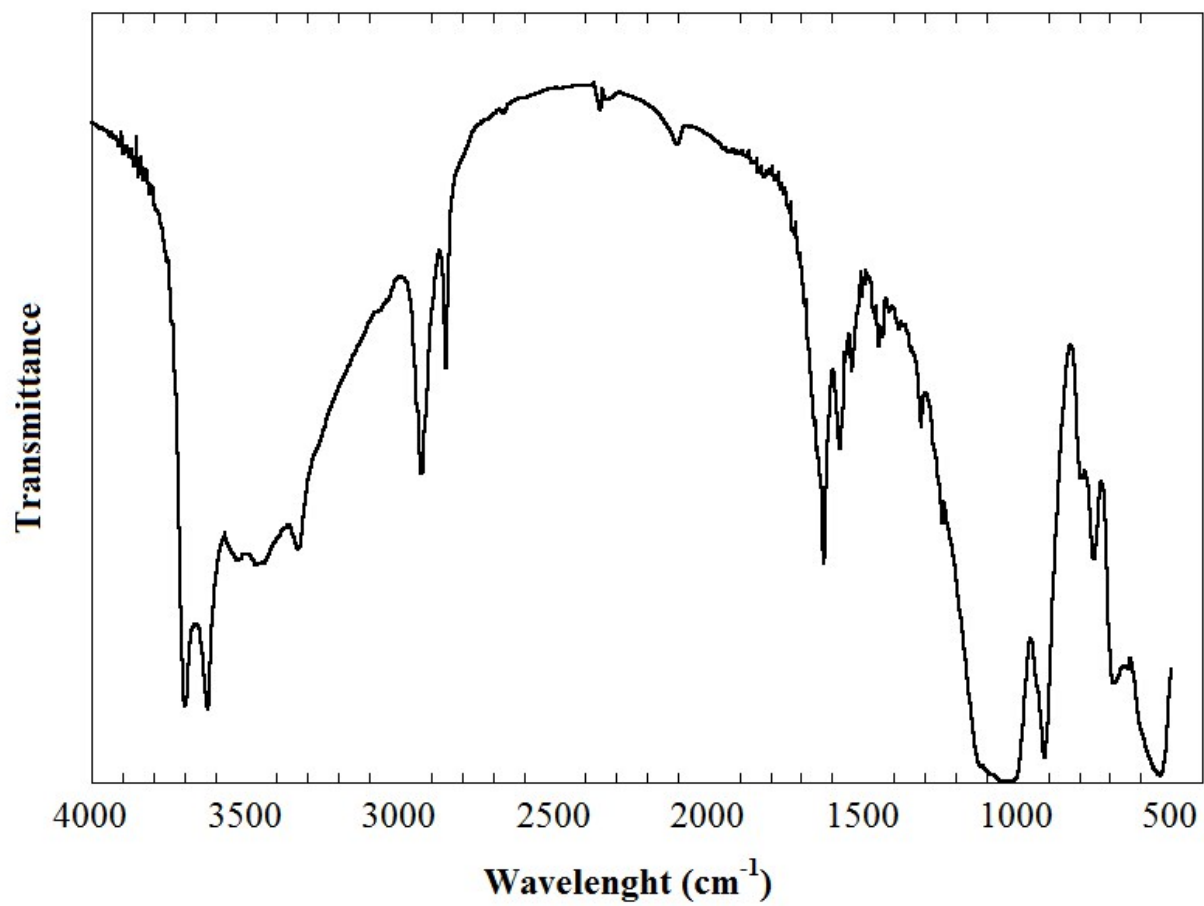


**Figure S1.** FT-IR spectrum of HNT-Trolox nanomaterial.

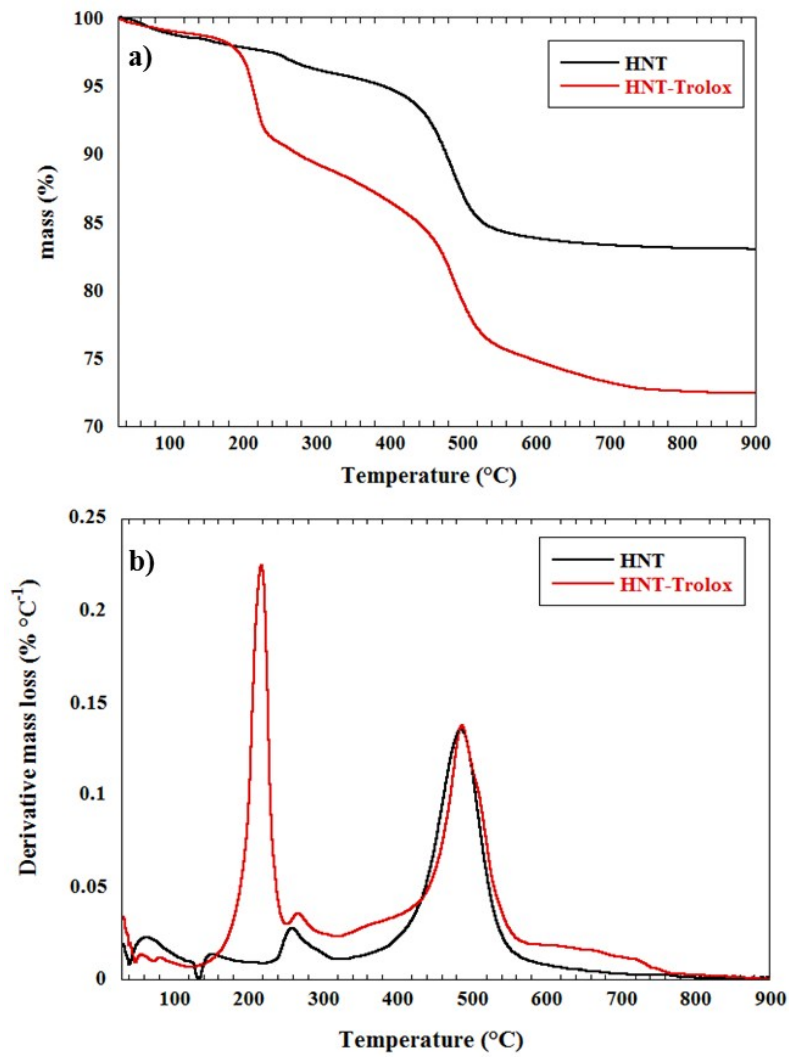


**Figure S2** Thermogravimetric (a) and derivative thermogravimetric (b) curves of HNT and HNT-Trolox nanomaterials.

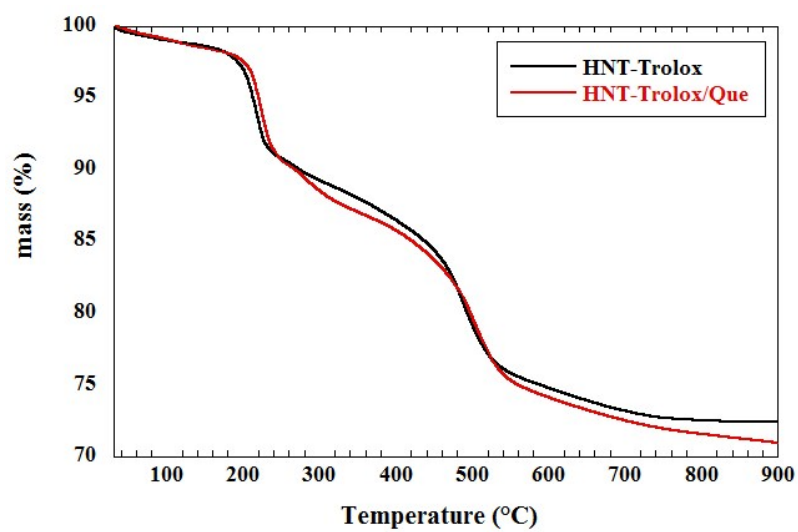


**Figure S3** Thermogravimetric curves for HNT-Trolox before and after quercetin loading.

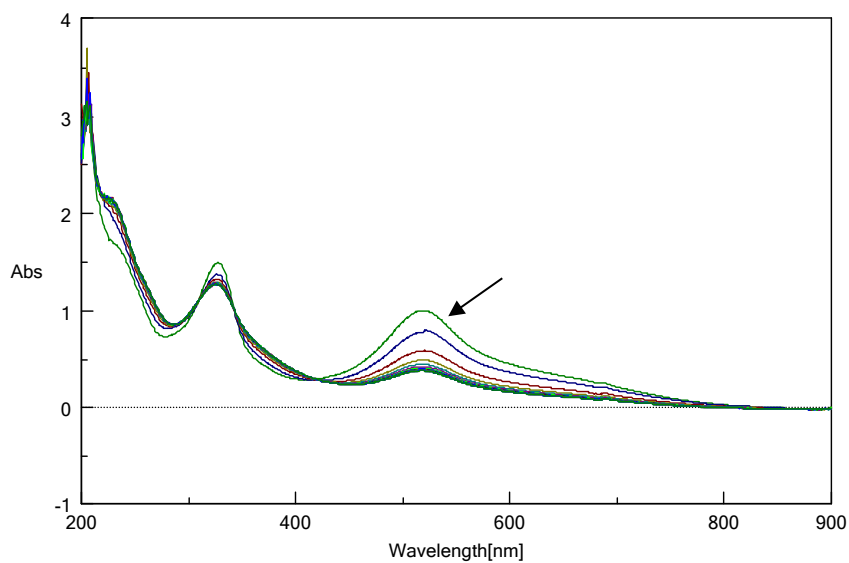


**Figure S4.** DPPH• absorption spectra upon reaction with Trolox; DPPH•:  $1.0 \times 10^{-4}$  M, Trolox:  $2.5 \times 10^{-5}$  M. The arrow indicates the spectrum of DPPH• before the addition of antioxidant.

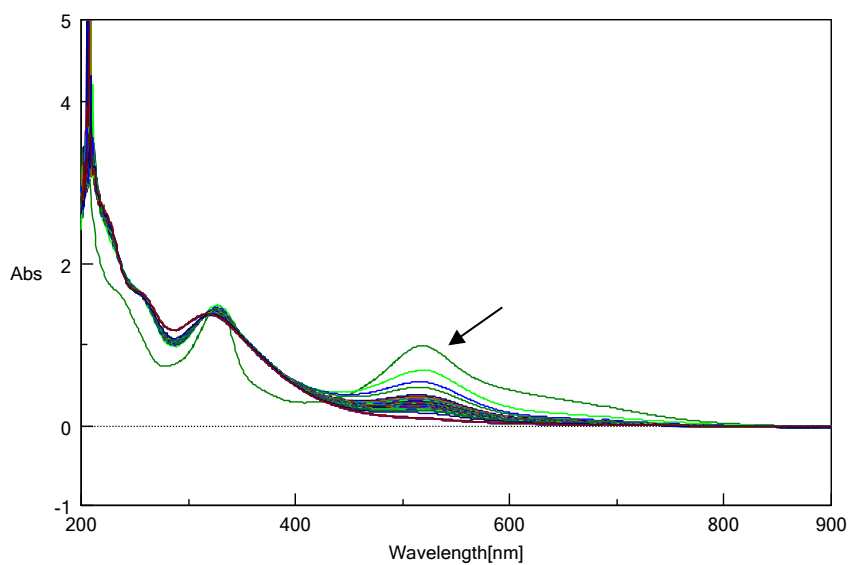


**Figure S5.** DPPH• absorption spectra upon reaction with quercetin; DPPH•:  $1.0 \times 10^{-4}$  M, quercetin:  $2.5 \times 10^{-5}$  M. The arrow indicates the spectrum of DPPH• before the addition of antioxidant.

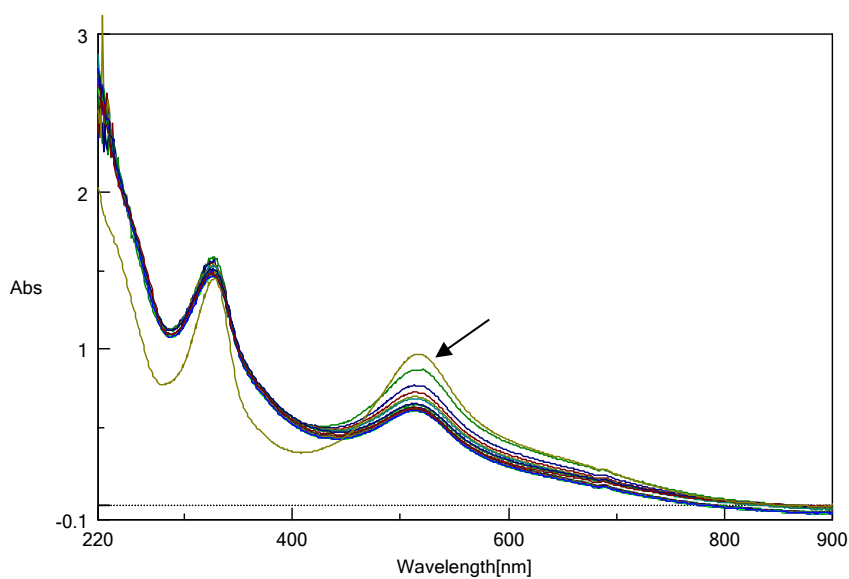


**Figure S6.** DPPH• absorption spectra upon reaction with HNT/Que; DPPH•:  $1.0 \times 10^{-4}$  M, HNT/Que:  $2.5 \times 10^{-5}$  M of loaded quercetin. The arrow indicates the spectrum of DPPH• before the addition of antioxidant.

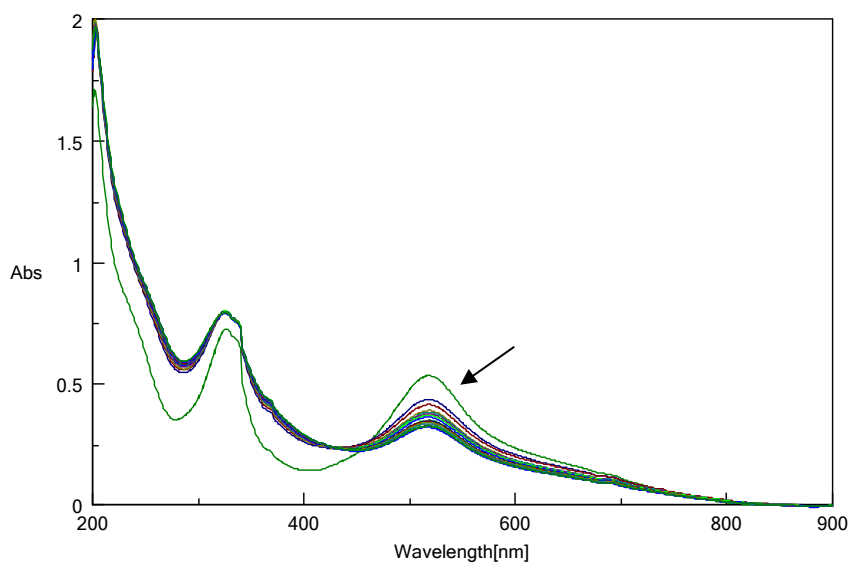


**Figure S7.** DPPH• absorption spectra upon reaction with HNT/Que; DPPH•:  $5.0 \times 10^{-5}$  M, HNT/Que:  $6.2 \times 10^{-6}$  M of loaded quercetin. The arrow indicates the spectrum of DPPH• before the addition of antioxidant.

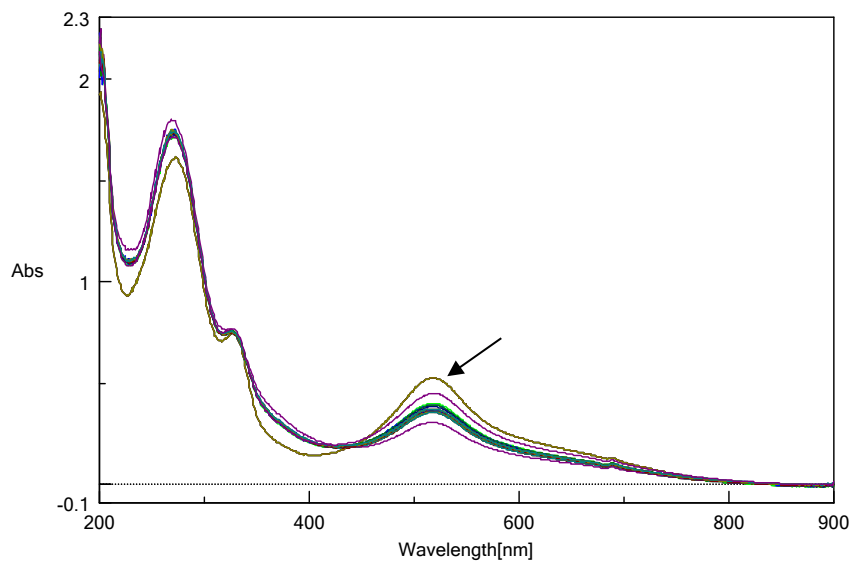


**Figure S8.** DPPH<sup>•</sup> absorption spectra upon reaction with HNT-Trolox/Que; DPPH<sup>•</sup>:  $5.0 \times 10^{-5}$  M, HNT-Trolox/Que:  $6.2 \times 10^{-6}$  M of loaded Trolox +  $1.7 \times 10^{-6}$  M of loaded quercetin. The arrow indicates the spectrum of DPPH<sup>•</sup> before the addition of antioxidant.

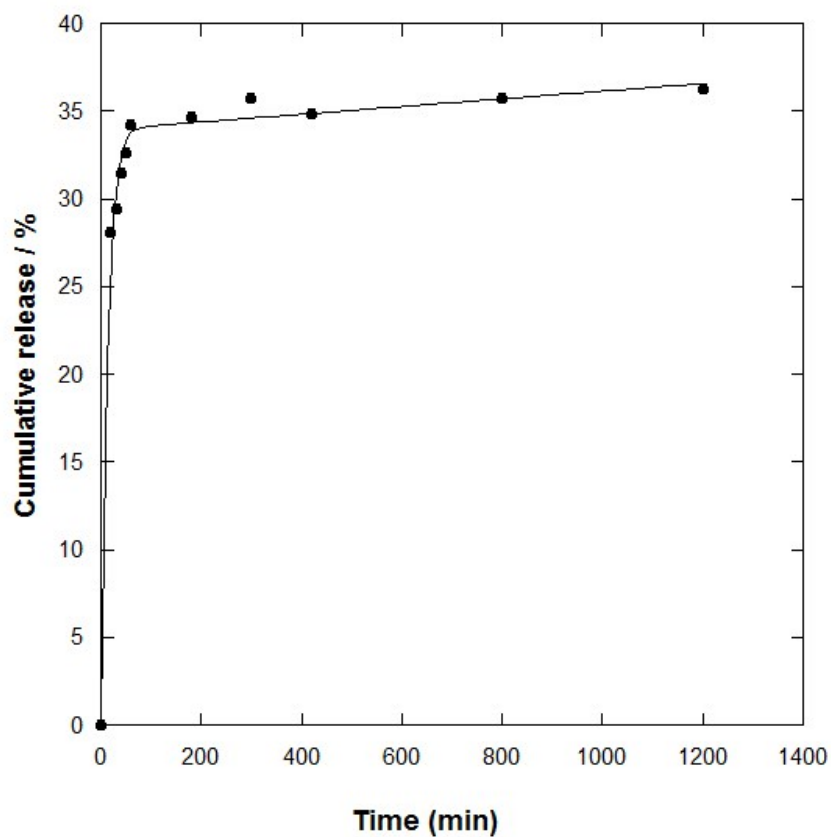
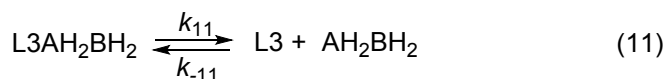
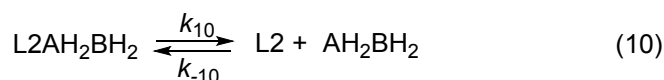
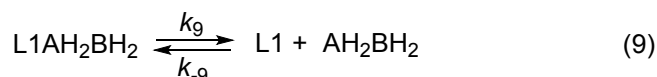
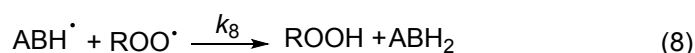
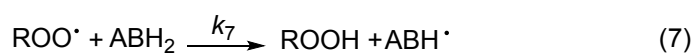
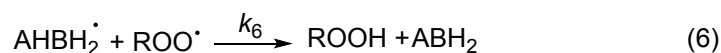


**Figure S9.** Release of quercetin from HNT/Que in acetonitrile, measured spectrophotometrically at 370 nm.

## Numerical fitting of O<sub>2</sub> consumption traces

In order to gain mechanistic insight into the antioxidant effect of HNT/Que, the oxygen consumption plots were analyzed by means of Gepasi (<http://www.gepasi.org>), a chemical simulation software able to reproduce the transient concentrations of intermediates during chemical reactions. The reaction scheme used to simulate the autoxidation inhibited by quercetin included into halloysite nanotubes is reported below (Equations 1-11).



Equations 1-4 describe the autoxidation of a generic oxidizable substrate (RH), that in our case is represented by cumene or styrene, whose propagation and termination rate constants are  $k_3$  and  $k_4$ , respectively, and are known from previous studies (see references in Table S1). The initiation rate

( $R_i$ ) is experimentally determined for each reaction condition ( $3.0 \pm 0.2 \times 10^{-9} \text{ M s}^{-1}$ ), while  $k_2$  is diffusion controlled ( $10^9 \text{ M}^{-1}\text{s}^{-1}$ ). Equations 5-8 represent the antioxidant effect of quercetin, which is described as a bifunctional compound ( $\text{AH}_2\text{BH}_2$ ) able to trap 4  $\text{ROO}\cdot$  radical, but with different efficiency for the two units. The rate constants for the reaction of the two units of quercetin with  $\text{ROO}\cdot$  radicals ( $k_5$ - $k_7$ ) are available from the studies performed in the absence of HNT, while  $k_6$ - $k_8$  are known to be fast reactions ( $10^8 \text{ M}^{-1}\text{s}^{-1}$ ) that occur at a nearly diffusion rate (E. T. Denisov, I. V. Khudyakov, *Chem. Rev.* **1987**, *87*, 1313–1357).

**Table S1.** Rate constants used for the fitting of the  $\text{O}_2$ -consumption plot.

	Rate constant ( $\text{M}^{-1}\text{s}^{-1}$ )	
	styrene <sup>[a]</sup>	cumene <sup>[b]</sup>
$k_3$	41	0.32
$k_4$	$2.1 \times 10^7$	$2.3 \times 10^4$

[a] J. A. Howard, K. U. Ingold, *Can. J. Chem.* **1965**, *43*, 2729-2736. [b] R. F. Enes, A. C. Tomè, J. A. S. Cavaleiro, R. Amorati, M. G. Fumo, G. F. Pedulli, L. Valgimigli, *Chem. Eur. J.* **2006**, *12*, 4646 – 4653

The release of quercetin from HNT is described by reactions 9-11. Several attempts were performed to properly simulate the  $\text{O}_2$ -consumption plots obtained from autoxidation experiments. In general, in both solvents in which it was studied, the quercetin release followed a two-phases process, comprising a fast release and a slower one. Although we succeeded in describing the autoxidation experiments by a two-sites model, the relative amount of quercetin released in the “fast” phase differed considerably depending on the solvent, being about 10% in chlorobenzene and about 40% in acetonitrile. In order to have a unique model for the antioxidant activity of HNT/Que, we combined information obtained experimentally in the two solvent systems and hypothesized that quercetin loaded on HNT is distributed into three sites, with low, medium and high affinity for



quercetin. The low affinity site (L1) contains 10% of the loaded quercetin and it is able to quickly release quercetin, either when the solvents are chlorobenzene or acetonitrile. The medium affinity site (L2) contains about 29% of quercetin, while the high affinity site (L3) contains the remaining 61%. From the numerical fitting of the experimental O<sub>2</sub>-consumption plots according to this 3-stages model, it is evident that the medium affinity site (L2) releases quercetin only when the solvent is acetonitrile. On the other hand, the high affinity site L3 gives a negligible release of quercetin in both solvents.

In Figure S10 and S11 the simulated release of quercetin from HNT, is calculated on the basis of the kinetic data obtained from numerical fitting of the experimental O<sub>2</sub>-uptake traces. In particular, we show the instantaneous quercetin concentration, and the overall percent released of quercetin during the time course of the autoxidation experiment.

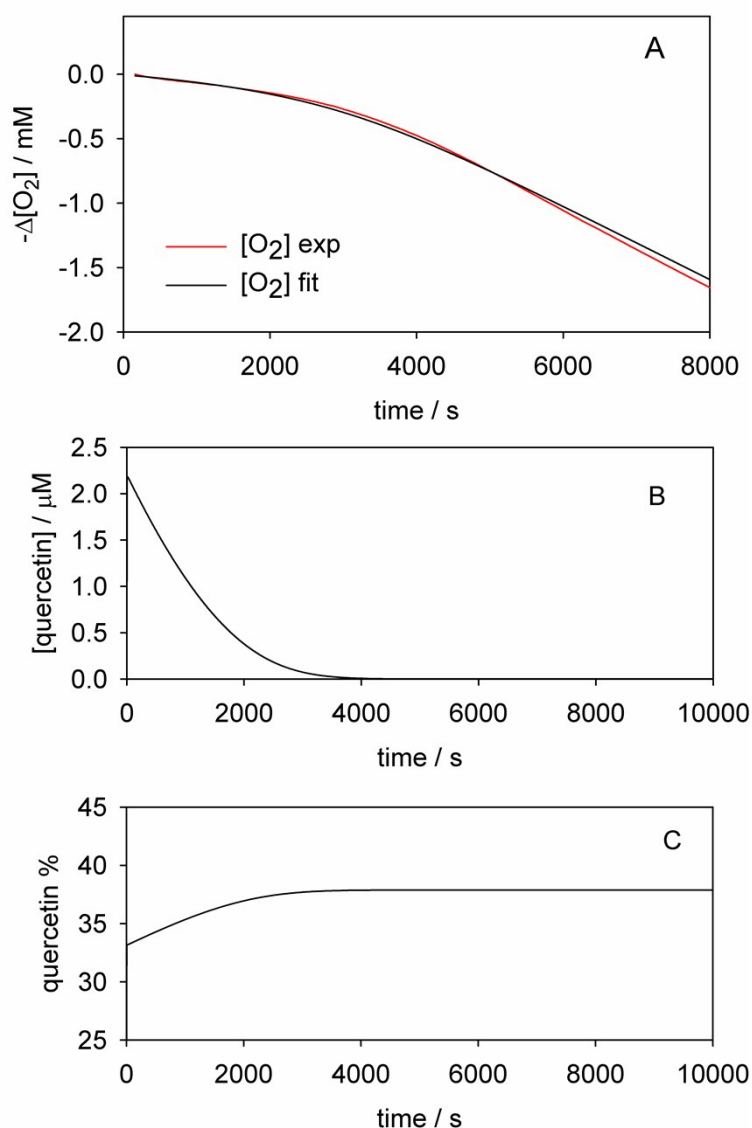


**Figure S10.** (A) Fitting of the  $\text{O}_2$  consumption plot measured during the autoxidation of cumene (3.5 M) in acetonitrile initiated by AIBN ( $2.5 \times 10^{-2}$  M) at  $30^\circ\text{C}$ , inhibited by HNT/Que corresponding to  $6.6 \mu\text{M}$  of quercetin. (B) Calculated instantaneous concentration of free quercetin in solution during the autoxidation. (C) Calculated cumulative percent release of quercetin during the autoxidation.

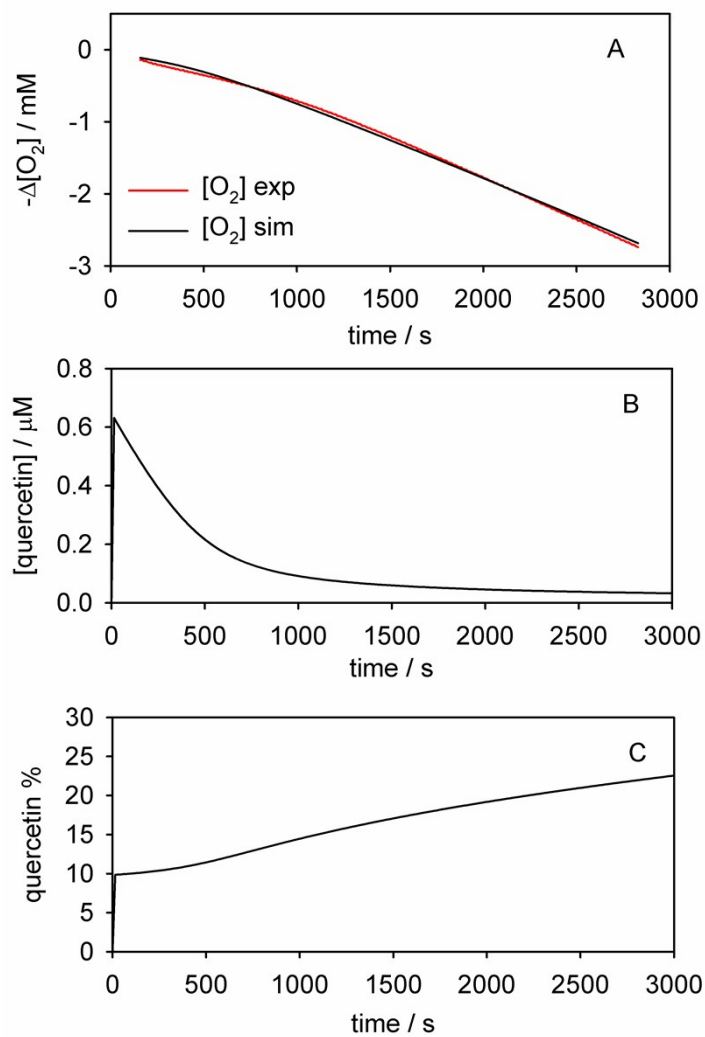


**Figure S11.** Results from the fitting of the  $\text{O}_2$  consumption plot measured during the autoxidation of styrene (4.2 M) in acetonitrile initiated by AIBN ( $2.5 \times 10^{-2}$  M) at  $30^\circ\text{C}$ , inhibited by HNT/Que corresponding to  $6.6 \mu\text{M}$  of quercetin. (A) Fitting of the  $\text{O}_2$  consumption. (B) Calculated instantaneous concentration of free quercetin in solution. (C) Calculated cumulative percent release of quercetin during the autoxidation.

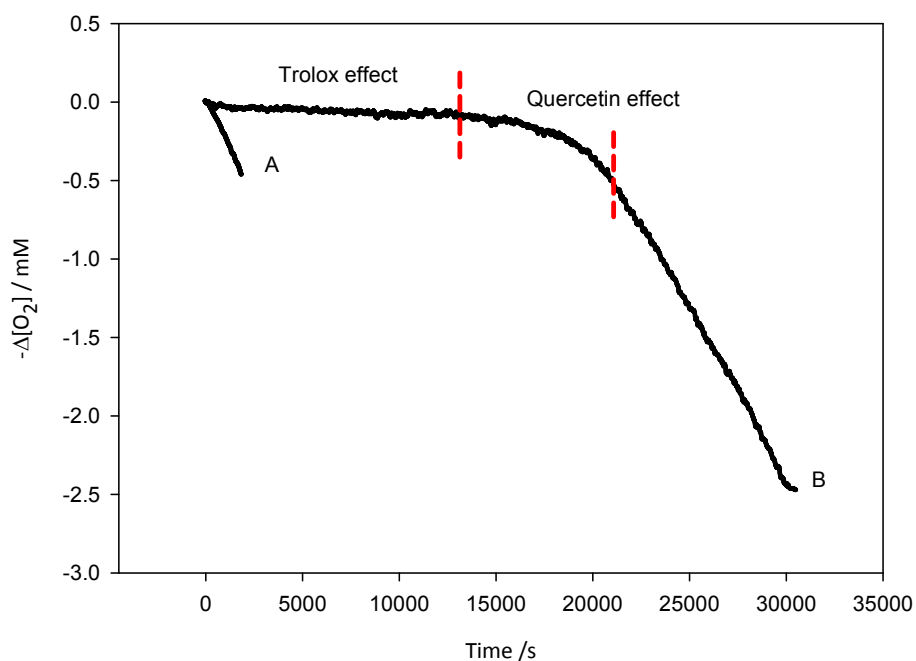


**Figure S12.** Representative oxygen consumption during the autoxidation of (A) cumene (3.6 M) initiated by AIBN (0.025 M) in ACN at 30° C in the absence of inhibitors; (B) or in the presence of Trolox  $2.5 \times 10^{-5}$  M and quercetin  $6.6 \times 10^{-6}$  M. The stoichiometric coefficient for the mixture is  $n = 1.8 \pm 0.1$ .

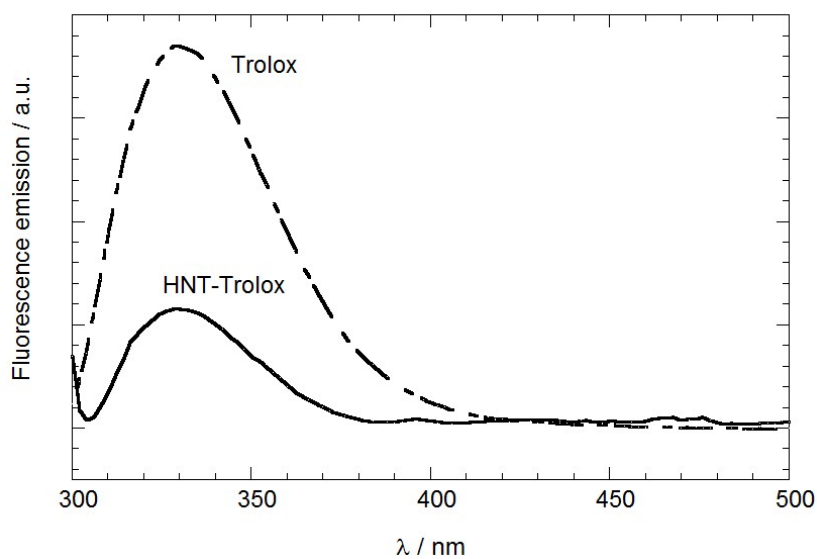


**Figure S13.** Fluorescence emission spectra for Trolox and HNT-Trolox hybrid in methanol.